AIAA-82-1240
Increased Capabilities of the Langley Mach 7 Scramjet Test Facility

S.R. Thomas and R.W. Guy, NASA
Langley Research Center, Hampton, VA

AIAA/SAE/ASME
18th Joint Propulsion Conference
June 21-23, 1982/Cleveland, Ohio

For permission to copy or republish, contact the American Institute of Aeronautics and Astronautics
1290 Avenue of the Americas, New York, NY 10104

INCREASED CAPABILITIES OF THE LANGLEY MACH 7 SCRAMJET TEST FACILITY

Scott R. Thomas* and Robert W. Guy**
NASA Langley Research Center
Hampton, Virginia

Abstract

An experimental research program which explored the potential for expanding the operating range of NASA Langley's Mach 7 Scramjet Test Facility is described. The facility uses electric arc-heated air as the test gas and is configured for testing airframe-integrated scramjet engine models at conditions duplicating flight velocities and temperatures. Previous scramjet testing in this facility was limited to a single simulated flight condition of Mach 6.9 at 115,300 ft. altitude. The present arc heater research demonstrated that the facility can be used for scramjet testing at simulated flight conditions from Mach 4 (at altitudes from 77,000 to 114,000 ft.) to Mach 7 (at altitudes from 108,000 to 149,000 ft.). Flow quality was established from the uniformity of measured total temperature profiles. In addition, nitrogen oxide levels in the test stream were determined for relating engine test data to expected flight performance. The test frequency and reliability of the facility were also improved by a novel redesign of the heater downstream electrode and by defining limits for stable arc operation.

Nomenclature

A^*	facility nozzle minimum flow area, or throat area
A_{eff}	effective facility nozzle exit flow area
D_{throat}	facility nozzle throat diameter
E	arc voltage
$h_{t,1}$	total enthalpy of facility airflow at the nozzle throat
I	arc current
$\dot{m}_{byp}$	mass flow rate of bypass air which is added downstream of the arc heater
$\dot{m}_{main}$	mass flow rate of main air which flows through the electric arc
M_∞	flight Mach number
M_1	airflow Mach number at the facility nozzle exit
NO	nitric oxide
NO_X	nitrogen oxides (except nitric oxide)
p_{HE}	total pressure of airflow in the arc heater
$p_{t,1}$	total pressure of airflow in the facility nozzle
P	arc power
R_{arc}	arc resistance
R_{bal}	ballast resistance
R_{total}	total electrical resistance, $R_{arc} + R_{bal}$
$T_{t,1}$	total temperature of airflow in the facility nozzle
ΔP	arc power fluctuation

Introduction

Development of airframe-integrated scramjet (supersonic combustion ramjet) technology continues to progress at NASA's Langley Research Center. The scramjet program focus is a fixed-geometry, hydrogen-burning, advanced engine concept (fig. 1) that has been shown to potentially be a very efficient propulsion device at flight speeds above Mach 4.[1,2] The integrated design uses the underside of the flight vehicle as part of the propulsion system; i.e., the forebody provides aerodynamic precompression of the flow entering the inlet, and the aft portion of the vehicle is used as part of the nozzle expansion surface. Prior to entering the scramjet module inlet, the freestream airflow is compressed by the vehicle bow shockwave. This feature reduces both the compression required from the scramjet inlet and the size of the scramjet module needed to produce the required thrust. The airflow, including the vehicle forebody boundary layer flow, enters the scramjet module inlet at a Mach number less than the flight Mach number because of the bow-shock precompression; however, the total enthalpy level (and total temperature) of the entering airflow corresponds to that of the flight Mach number.

Experimental work in support of this scramjet concept includes inlet configuration tests, direct-connect combustion tests, and subscale engine tests. Inlet tests have been conducted in several Langley aerodynamic facilities,[3,4] while the direct-connect combustion tests have been conducted in a vitiated air (hydrogen-combustion-heated with oxygen replenishment) facility at Langley (for example, see refs. 5 and 6.) Scramjet engine tests at a simulated flight Mach number of 4 have been conducted in vitiated air facilities at the General Applied Science Laboratories (GASL) in Westbury, N.Y. and at Langley.[7,8] Engine tests at a simulated flight Mach number of 7 have been conducted in the GASL facility and in electric-arc-heated air at the Langley Mach 7 Scramjet Test Facility.[8] These engine test facilities are different from most aerodynamic wind tunnels because they must provide simulation of engine-airframe integration effects such as vehicle bow shock precompression and boundary layer ingestion by the scramjet. The total enthalpy corresponding to the simulated flight Mach number is duplicated, and tests are conducted at total pressures which simulate practical flight altitudes. The flight vehicle bow shock precompression is simulated by testing at a tunnel Mach number less than the Mach number which corresponds to the tunnel flow total enthalpy. Flight vehicle boundary layer ingestion is partially simulated by mounting the scramjet model so that the facility

*Aerospace Engineer, Engine and Components Group, Hypersonic Propulsion Branch, High-Speed Aerodynamics Division, Member AIAA

**Leader, Engine and Components Group, Hypersonic Propulsion Branch, High-Speed Aerodynamics Division

This paper is declared a work of the U.S. Government and therefore is in the public domain.

nozzle boundary layer approaching the model top surface is ingested.

This report describes an arc heater research test series which expanded the test capability of NASA Langley's Mach 7 Scramjet Test Facility. This effort involved operating the facility over a wide range of conditions that had not been used prior to this test series. In the past, the facility was operated at a single Mach 7 test condition. Specifically, the potential for expanding the operational capability of the facility for testing over a range of simulated flight conditions at Mach numbers from 4 to 7 was demonstrated. This increased capability will allow a complete test program to be conducted over this Mach number range without removing the model from the facility. Test flow quality is evaluated from total temperature profiles and nitrogen oxide content is documented so that future engine test data from the facility can be properly related to actual flight conditions. Solutions to arc stability and arc heater O-ring problems, which had limited facility productivity in the past, are discussed.

The Langley Mach 7 Scramjet Test Facility

The Langley Mach 7 Scramjet Test Facility (STF) is an electric arc-heated facility with air as the test gas.[9,10] Figure 2 shows an elevation view of the tunnel circuit. Major support systems of the STF include a 5000 psig air supply, a 20 MW dc electrical power system, a 1400 psig deionized cooling water system, a 100 ft. diameter vacuum sphere with a 3-stage steam ejector evacuation system, a 750 psig gaseous hydrogen fuel supply, and a 3000 psig hydraulic model injection system. These systems are described in more detail in reference 9.

Longitudinal section views of the electric arc heater and the plenum chamber are shown in figures 3 and 4, and a schematic of the arc heater electrical circuit is shown in figure 5. Electric power is provided by two dc power supplies connected in series with the arc heater and with two sets of ballast resistors which are used to achieve arc stability. The power supplies, which consist of arrays of ac transformers and silicon diode rectifiers can be regulated to provide various power levels (up to 20 MW) to the arc heater circuit. The actual specification of the power level is obtained by selection of power supply transformer output voltages which are termed "tap settings". Each power supply has 33 available tap settings.

The electric arc is initiated by using a 0.035 in. diameter steel rod to make contact between the two coaxial cylindrical electrodes (upstream and downstsream electrodes). The electrodes are separated by the electrically-insulated main air-inlet chamber (fig. 3). The arc establishes between the electrodes and, except for the termination regions, is confined along the heater centerline by the vortex flow of the main air stream, which is purposely injected with a tangential velocity (swirled in). This type of arc heater is termed a vortex-stabilized arc heater.[11] The arc termination regions (where the arc attaches to the electrodes) are continuously rotated by a combination of the air swirl and interaction of the arc with the externally-applied magnetic fields. The arc rotation spreads the intense heating rate of the arc attachment regions over much greater surface areas and thereby prevents the copper electrodes from melting in these regions. The external magnetic field, which is produced by the water-cooled magnetic field coils, also aids in stabilizing and containing the arc.

The arc-heated air is mixed in the plenum chamber with an unheated bypass airstream to form a resultant test stream with the desired stagnation conditions. This mixing scheme is necessary because the arc heater cannot process the total facility air flow and maintain a stable operating mode. The bypass air is injected radially from two sets of slots machined in the 2nd and 3rd plenum rings (fig. 4). The radial injection enhances mixing and also breaks up the swirl downstream of the arc heater to improve flow quality for engine testing. This test gas mixture is expanded through a contoured nozzle into the test section. The flow is then diffused to subsonic velocity, cooled by an aftercooler, and exhausted into a vacuum sphere (fig. 2).

Arc Heater Research Tests

Several modifications to the STF (fig. 6) have recently been completed which will improve future testing capability. These include a new Mach 6 contoured nozzle, test section modifications to provide better flow visualization and model access, new computer-operated hydrogen fuel controls, a pyrophoric ignitor fuel[12] system, and improvements to the facility diffuser. However, the most significant improvement in terms of facility test capability was the structural strengthening of the arc heater and plenum chamber. This permitted an increase in maximum facility stagnation pressure from 30 to 45 atm. With this new capability, a program was initiated to determine the feasibility of conducting scramjet engine tests in the STF with duplication of flight velocities and temperatures over a simulated flight Mach number range of 4 to 7 at several simulated altitudes. This would require facility operation over a wide range of arc powers, air flow rates, and heater and plenum stagnation pressures. Unfortunately, the operating characteristics of the arc heater/electrical system combination were known only for the previous single test point ($P = 9.77$ MW, $p_{t,1} = 28.5$ atm., $T_{t,1} = 3925^{\circ}$R, etc. as tabulated in reference 9).

Operating conditions at other test points could not be accurately predicted because arc heaters are generally not well understood on a theoretical basis. Although the results of previous research on similar types of arc heaters may be useful to approximate the trend of operational characteristics due to parameter changes, every arc heater when coupled with a particular power supply has some unique operating characteristics. To determine these characteristics, an experimental research program must be conducted with that arc heater/power supply combination. The arc heater research test series was such a program. The purpose of the test series was to demonstrate the potential of the Scramjet Test Facility to produce flow conditions useful for scramjet engine testing at simulated flight Mach numbers from 4 to 7 and to determine the arc heater/electrical system operational characteristics.

In addition to test setup variables such as power supply tap setting, ballast resistance, and air flow rate, facility nozzle throat area is an important parameter when determining arc heater operating characteristics. The pressure within the arc heater and plenum chamber is strongly dependent on the facility nozzle throat area where the test stream is always sonic or "choked;" consequently, the size of this throat will significantly affect these operating conditions, providing the main air flow exiting the downstream electrode is not choked. Therefore, results of previous scramjet tests[7,8] were used to determine approximate specifications for facility contoured nozzles (i.e., exit Mach number, exit area, and, therefore, throat area) useful for testing scramjet engine models typically 8 in. high by 6.4 in. wide at simulated flight Mach numbers of 4, 5.5, and 7. (See fig. 7.) The facility nozzle exit area at each simulated flight Mach number has to be large enough to accommodate this size model and avoid the possibility that waves originating at the free jet nozzle exit might affect measurements of engine thrust, pressures, etc. Therefore, each nozzle has a different throat area. During the test series, the size of the nozzle throat, both the main and bypass airflow rates, the power supply tap settings, and the ballast resistance were varied to generate a wide range of heater test conditions.

Special Test Apparatus

For certain conditions in earlier test programs, the electric arc had become unstable and struck tunnel components downstream of the end of the downstream electrode, resulting in some damage to those components (plenum rings, nozzle throat, etc.). To eliminate risk to expensive contoured tunnel nozzles during the test series, temporary, converging metering nozzles and a constant area, uncooled connector duct (coated internally with zirconium oxide) were used. This test setup is shown schematically in figure 8. Since the flow velocity at the nozzle throat is sonic, the conditions of the flow downstream of the throat have no effect on those in the plenum chamber and the arc heater. Therefore, testing with converging metering nozzles of circular cross-section with the same throat areas, but without the complex expansion contours of a tunnel nozzle, allows proper arc heater operation at the desired test conditions. Metering nozzles with three different throat sizes were used (fig. 7): a 1.3 in. diameter throat for simulating Mach 7 flight conditions, a 2.2 in. diameter throat for simulating Mach 5.5 flight conditions, and a 5.6 in. diameter throat for simulating Mach 4 flight conditions.

Measured Parameters

Parameters which were measured to establish test conditions included arc voltage and current; main and bypass air mass flow rates; cooling water flow rates to all heater components, the plenum rings, the plenum, and the throat; inlet and outlet cooling water temperatures to the same components; heater pressure; and plenum chamber pressure. From these measurements, which were recorded 20 times per second, heater electrical operating characteristics were determined, and heater and test flow total enthalpies were calculated according to the energy balance equations given in reference 9.

During some of the tests, nitrogen oxide levels and flow total temperatures were measured at the exits of the metering nozzles (fig. 8). The nitrogen oxide levels were determined from spectroscopic analysis of samples of the test flow obtained in a sample bottle using an instream probe. For tests with total temperatures below 2500°R, temperature profiles were obtained using a 9-probe chromel-alumel thermocouple rake. For tests with total temperatures above 2500°R, a single centerline temperature measurement was obtained using an iridium/iridium-40 percent rhodium thermocouple. Velocity, conduction, and radiation errors were minimized by the thermocouple probe design.[13]

Test Results

As a result of these tests, much was learned about the operating characteristics of the facility and its potential for scramjet engine testing over a broadened range of test conditions. Maps of this range, in terms of total pressure and total enthalpy, are presented for three potential facility nozzles. Operational problems, including heater O-ring failure and arc instability, are discussed, and solutions and limits of operation are presented. Arc heater/power supply electrical characteristics, including arc voltage, arc current, and arc resistance, are presented and the effects of ballast resistance, airflow rate, and pressure on these characteristics are discussed. Measured total temperature profiles are analyzed to assess flow quality for future scramjet tests over a range of simulated flight Mach numbers. Measurements of nitrogen oxide contaminants in the arc-heated flow are presented for a range of test conditions for use in relating facility scramjet performance to actual flight performance.

Expanded Test Capability

Results from a large number of tests indicated that the facility test conditions of interest could be obtained with the following arc heater/electrical system configuration: equal tap settings on both power supplies, a total ballast resistance of 1.304 ohms, and a new downstream electrode design (to be discussed later). The versatility of this configuration was demonstrated through successful facility operation over a wide range of test conditions at arc powers from 2.3 to 12.7 MW. The test conditions which resulted in a stable operating mode and which are useful to reproduce during future engine and component tests are shown in figures 9, 10, and 11 for the 1.3 in. diameter throat, the 2.2 in. diameter throat, and the 5.6 in. diameter throat, respectively. Total enthalpies above and below the ranges of data shown are possible in the facility, but are not presently of interest in the scramjet program.

The test capability of most immediate interest is the facility operating range available for testing the subscale scramjet engine models. Scramjet engine tests will be meaningful only at enthalpy levels simulating flight Mach numbers equal to or greater than the facility nozzle exit Mach number, which is equal to the scramjet inlet Mach number. These conditions are shown to the right of the dashed vertical lines on figures 9, 10, and 11. Testing in this region represents a flight situation where the freestream flow is compressed by the

vehicle bow shockwave prior to entering the scramjet. The degree of forebody precompression that is simulated by the facility increases as total enthalpy is increased above the level corresponding to the facility nozzle exit Mach number. Flight conditions based on values of precompression which have been chosen for the present study and others[7,8] are represented by the total enthalpies indicated by the solid vertical lines in figures 9, 10, and 11; these lines correspond to flight Mach number simulations of 7, 5.5, and 4, respectively. The range of test stagnation pressure for each of these simulated flight Mach numbers is shown on the figures.

The new flight Mach number - altitude operational envelope for the STF (corresponding to the solid vertical lines in figs. 9-11) is shown in figure 12. The demonstrated potential of the facility for scramjet engine testing extends from simulated flight conditions of Mach 4 (at altitudes from 77,000 to 114,000 ft.) to Mach 7 (at altitudes from 108,000 to 149,000 ft.). It must be noted that only heater operation has been demonstrated at the Mach 4 - 77,000 ft. altitude point shown in figure 12; some minor air piping system changes in the facility must be made to obtain the bypass airflow rate required to duplicate the correct plenum total pressure and enthalpy. The shaded symbol on figures 9 and 12 represents the single point operation of the STF prior to these arc heater research tests.

Operational Problems

Critical O-ring problem.- A very important operational problem, which was eliminated during this test series, was the failure of a critical O-ring after every high arc power test (with an arc power greater than approximately 7.5 MW). The O-ring provides a seal between the high pressure cooling water and the facility airflow at the downstream end of the downstream electrode (fig. 13).

With the original downstream electrode configuration, the tip of the electrode was some distance from the cooling water passage, as shown in figure 13, and was directly exposed to the hot airflow exiting the downstream electrode (entering the plenum chamber). During a hot test, the high temperature airflow caused the downstream electrode to thermally expand. The tip of the electrode extended even farther from the cooling water passage and became very hot. After the test was terminated, the downstream electrode contracted and dragged the hot tip over the O-ring surface. For every high power test, the combination of this sliding motion and the high temperature of the electrode tip caused O-ring damage which resulted in cooling water leaking into the air passages of the arc heater. Therefore, the O-ring had to be replaced after every test.

The problem was eliminated by redesign and modification of the downstream electrode tip. The new design, shown in figure 14, constricted the tip to a smaller internal exit diameter to allow space for a cooling water passage between the O-ring and the hot airflow. This cooling water passage also moves with the tip as the electrode grows thermally and maintains the surface in contact with the O-ring at a reasonably-cool temperature at all times. The modification completely resolved the problem. At the completion of this test series, 125 tests, 50 of which were at high arc power, had been completed without O-ring damage. A photograph of the new downstream electrode configuration is shown in figure 15.

Arc instability.- An arc instability problem, characterized by significantly-increased fluctuations in arc power and arc attachment further downstream than normal, was observed for some test conditions during the test series as well as during earlier test programs. This problem occasionally resulted in damage to the tip of the downstream electrode; and, in a few cases, the arc attached downstream of the electrode, causing damage to the plenum rings or to the metering nozzle flange. This test series effectively solved the arc instability problem by defining run conditions which resulted in a stable operating mode.

Maximum arc power fluctuations normalized by the corresponding mean arc powers are shown in figure 16 as a function of arc resistance-to-total resistance ratio for various run conditions. Curves are presented for data obtained using the original downstream electrode with the 1.3 in. diameter throat and using the new constricted downstream electrode with all three metering nozzles. Data obtained with some of these configurations exhibited considerable scatter; therefore, only curves which were faired through the mean of the data are shown. The normalized power fluctuations were relatively constant for all electrode-throat combinations below an arc-to-total resistance ratio of 0.65. However, the power fluctuation with both electrodes increased dramatically at higher resistance ratios. For the operational range explored in this test series, the arc was considered to be stable if arc resistance remained below approximately 65 percent of the total resistance (ballast resistance plus arc resistance). At greater arc-to-total resistance ratios, the arc was less stable and the runs were often erratic with large arc power fluctuations sometimes causing damage. Thus, the data emphasize the importance of maintaining sufficient ballast resistance (relative to the arc resistance) for stabilizing the arc and minimizing power fluctuations. For all run conditions, the output power fluctuations were smaller when operating with the new constricted downstream electrode design than with the original downstream electrode design and also decreased as metering nozzle diameter was increased. The arc was contained within the downstream electrode and no damage to the downstream electrode, plenum rings, or metering nozzle flange occurred due to an arc instability problem after the new design downstream electrode was placed in service.

Solutions to the O-ring problem and the arc instability problem were very important results of the test series. Solving the O-ring problem substantially increases the potential productivity of the STF for any type of test program by eliminating O-ring failure and, therefore, the need to service the arc heater between tests. Defining the limits of arc stability and establishing systematic set-up procedures to assure stable operation eliminates the expense of refurbishing hardware which was occasionally damaged by the arc and has increased the dependability and consistency of the facility.

Arc Heater Electrical Characteristics

During the test series, power supply tap

setting, ballast resistance, air mass flow rates, and throat size were systematically varied to define the electrical operating characteristics of the arc heater/electrical system combination in the range of interest. The amount of ballast resistance in the arc heater circuit was varied between approximately 1.304 and 1.594 ohms. As expected, lower ballast resistance resulted in higher arc power at a particular power supply tap setting as shown in figure 17. The increased arc power permits lower flight altitudes to be simulated; however, sufficient ballast resistance must be present in the arc heater circuit to maintain stable operations. A ballast resistance of 1.304 ohms was determined to be sufficient to maintain stable arc operation while achieving any operating condition in the range of interest with the new downstream electrode design installed. Therefore, all electrical data shown here were obtained using this value of ballast resistance.

A general criterion adopted for setting up the majority of the tests in the series was to maintain the total enthalpy of the flow exiting the arc heater at the previous level ($\approx$ 3500 BTU/lbm) regardless of the arc power level or the desired test flow total enthalpy. Therefore, the required "nominal" air mass flow rate through the arc heater for a particular arc power level was determined by ratioing the attempted arc power to the previous single point operation power level (9.77 MW, see ref. 9) and using a proportional main air mass flow rate. However, on some tests, the main air mass flow rate was increased as much as 100 percent above the nominal value to examine the effect of main airflow rate on arc heater performance. Figure 18 illustrates the effect of both main air flow rate and facility nozzle throat size on arc resistance. The data in this figure were obtained with each of the three metering nozzles while maintaining constant tap settings of 16 on both power power supplies. The nominal main airflow rate was 1.22 $\frac{\text{lbm}}{\text{s}}$. Generally, increased main airflow rate yields increased arc resistance while increased facility nozzle throat area (which results in decreased plenum and heater stagnation pressures) leads to decreased arc resistance. This type of data demonstrated that the nominal main air flow rates for the various arc power levels were sufficient to generate the operational conditions of interest with the 1.3 in. diameter metering nozzle. Main air flow rates greater than the nominal values were not desirable because the resultant increase in arc resistance quickly led to less stable arc behavior. However, during tests with the larger throats, increasing the main airflow rates above the nominal level was possible (since arc resistance was lower) and, in fact, was necessary to achieve maximum arc power at the highest power supply tap setting. Nominal values of main air flow were generally used with the larger throats at power supply tap settings below 33.

Arc heater electrical operating characteristics are presented in figures 19 through 23. For a particular ballast resistance and power supply tap setting, these characteristics are a function of main air mass flow rate and heater pressure. Heater pressure is affected by main airflow rate and by both throat area and bypass air flow rate when the flow at the exit of the downstream electrode is not choked. Therefore, for simplicity, the electrical characteristics shown are for a ballast resistance of 1.304 ohms and nominal airflow rates. Nominal main airflow rate has previously been defined. Nominal bypass airflow rate is that required at each arc power level to achieve the test total enthalpy corresponding to the simulated flight Mach number.

Power supply tap settings and the nominal main air mass flow rates required to achieve various arc power levels are shown in figures 19 and 20, respectively, for the three nozzle throat sizes. At a given tap setting, arc power decreases as metering nozzle diameter increases. At the highest tap setting (tap 33 on both power supplies), only 11.08 MW of arc power was obtained with the 5.6 in. throat while 12.74 MW was obtained with the 1.3 in. throat at the same main airflow rate. Higher arc power with the larger throats had to be achieved by increasing main airflow rate above the nominal value and increasing arc resistance as shown in figure 18.

Arc voltage, arc current, and arc resistance as functions of arc power for the run conditions defined in figures 19 and 20 are shown in figures 21, 22, and 23, respectively. The magnitude of these parameters generally increase with increasing arc power. Operation with larger throat sizes and, therefore, reduced plenum and heater pressure, resulted in lower arc resistance and arc voltage but a higher arc current at a particular arc power level.

For a given test setup condition, i.e., main air flow rate and arc power supply tap setting, the arc heater electrical properties (figs. 19-23) change with increasing throat size until a choked flow is established at the exit of the downstream electrode. Once the electrode flow is choked, a further decrease in the plenum pressure as the throat size is increased has no effect on the heater electrical and fluid mechanical properties. During the present test series, the flow was choked only when using the 5.6 in. diameter throat. However, a significant pressure drop was observed between the downstream electrode and the plenum chamber during operation with the 2.2 in. diameter throat, and, therefore, a choked flow would be expected with a throat size between the 5.6 in. diameter and the 2.2 in. diameter. The variations in electrical properties observed (figs. 19-23) when changing throat size from 2.2 in. diameter to 5.6 in. diameter are much less than those observed when changing throat size from 1.3 in. diameter to 2.2 in. diameter. This indicates that the effect of increasing throat area on arc heater electrical characteristics becomes less significant as the flow from the downstream electrode approaches a choked condition.

Total Temperature Profiles

Total temperature profiles were measured at the exits of the metering nozzles during the test series to determine if the flow uniformity was sufficient to warrant constructing facility contoured nozzles for testing scramjets at simulated flight Mach numbers of 4 and 5.5 (a nozzle for Mach 7 flight simulation exists). Concern about flow uniformity stems largely from the facility air injection configuration where the unheated bypass air is injected into the arc-heated flow at the exit of the downstream electrode. To achieve a satisfactory test flow, a high degree of mixing

must occur in the plenum before the flow is expanded in the facility nozzle.

During a previous test series,[9] pitot pressure and stagnation point heating-rate surveys at the exit of the facility contoured nozzle were used to obtain a total enthalpy profile and establish the uniformity of the flow for Mach 7 scramjet engine testing (see fig. 12 in ref. 9). In the present test series, only centerline total temperatures were measured at the exit of the 1.3 in. diameter metering nozzle. At Mach 7 enthalpy levels, these temperatures were somewhat lower than those derived from the energy balance measurement of total enthalpy. Although thermocouple results are subject to numerous errors at the Mach 7 total temperature level ($\approx 4000^{\circ}$R), the flow is probably well-mixed since the centerline temperature is less than the bulk temperature estimate.

To explore the flow uniformity of the facility test stream for testing at simulated Mach 5.5 flight conditions, total temperature surveys were measured at the exit of the 2.2 in. diameter metering nozzle throat using a chromel-alumel thermocouple rake. Tests were made with the rake rotated from 0° to 135° in 45° increments to obtain profile data across the entire nozzle exit area. Total temperature profiles obtained with a flow total pressure representative of flight at an altitude of 91,000 ft. (fig. 24), indicate that the flow uniformity was exceptionally good. Therefore facility operation at this simulated Mach 5.5 flight condition is adequate for scramjet testing. Bulk total temperature derived from the energy balance technique was in excellent agreement with the thermocouple measurements.

To explore the flow uniformity of the facility test stream for testing at simulated Mach 4 flight conditions, total temperature surveys were measured at the exit of the 5.6 in. diameter metering nozzle using the chromel-alumel thermocouple rake. The chance of poor flow uniformity due to inadequate mixing of the arc-heated main airflow with the unheated bypass airflow within the plenum chamber was greatest with the 5.6 in. diameter throat because the bypass air was injected into a choked main airflow issuing from the constricted downstream electrode. In the case of the smaller two throats, the flow from the downstream electrode was not choked.

Total temperature profiles obtained using the 5.6 in. diameter metering nozzle are shown in figure 25. Flow total pressure was representative of Mach 4 flight at 91,000 ft. altitude. The open symbol data were obtained with bypass air injected from both injection stations as shown in figure 14. Large total temperature variations across the nozzle exit and asymmetry in the profiles obtained were noted as the thermocouple rake was rotated from 0° to 135°. To correct these problems, the injectors at the upstream bypass air injector station (fig. 14) were enlarged and all of the bypass air was injected from this station. This technique permitted the bypass air to be injected closer to the supersonic flow exiting the downstream electrode. The corresponding total temperature profile, obtained only for the 135° rake orientation, is shown by the shaded symbols in figure 25. It indicates that much improved mixing occurred between the arc-heated air and the bypass air. The flow was still less uniform than that obtained with the 2.2 in. diameter metering nozzle; however, the maximum variation of total temperature from the arithmetic average value was only ±4 percent. This uniformity is considered to be adequate for scramjet engine testing. More uniform flow should be attainable by redesigning and fabricating new air injection components to replace the existing plenum rings so that all bypass injection would take place even closer to the main air stream exiting the downstream electrode.

The total temperature profile data shown in figures 24 and 25 specifically indicate the facility flow uniformity for only two points in the STF test envelope (fig. 12), i.e., simulated flight Mach numbers of 5.5 and 4, respectively, at a simulated altitude of 91,000 ft. However, temperature profiles from other tests, some simulating other altitudes and some exploring the effect of varying the quantity of bypass air which is injected, indicate that altitude simulation has little effect on flow uniformity. These results show that flow conditions in the STF are adequate for scramjet testing over a simulated flight Mach number range from 4 to 7 and a range of simulated altitudes. Tests at selected Mach numbers within the STF test envelope (fig. 12) can be accomplished without removing the model from the facility by simply changing the facility nozzle.

Nitrogen Oxide Contaminants

Nitrogen oxide contaminants in the test stream entering a scramjet engine not only affect the ignition of the hydrogen-air mixture[14] but also affect engine performance by reducing the oxygen available for the combustion process.[15] Therefore, a knowledge of the quantity of nitrogen oxides in the flow is necessary so that engine test results from ground facilities can be properly related to actual flight situations where the nitrogen oxides would not be present. In the present tests, flow samples for several test conditions using all three metering nozzles were captured in a gas sample bottle and analyzed using a mass spectometer. Total enthalpies corresponding to Mach 4, 5.5, and 7 flight were duplicated with the proper throat installed. At each enthalpy level, facility arc power and air mass flow rate were varied to achieve a range of total pressure and, therefore, a range of altitude simulation. It must be noted that some copper oxide contaminants from the arc heater electrodes are also present in the flow; however, the levels were not measured during these tests.

The results of these nitrogen oxide measurement tests are shown in figure 26. Generally, nitrogen oxide level increases as Mach number simulation, i.e., flow total temperature, is increased from 4 to 7. This trend is most pronounced at the lower arc powers (lower total pressure or higher simulated altitudes). For all of the data shown in figure 26, the total enthalpy of the flow leaving the downstream electrode was essentially constant. Also, most of the nitric oxide present in the flow was produced in the heater. Therefore, lower percentages of nitrogen oxides would be expected at the test total enthalpies corresponding to lower Mach numbers because of the dilution effect of the higher bypass air flows required to achieve these enthalpies.

The levels of nitrogen oxide contamination shown in figure 26 are significant; reaching a maximum of more than 3.5 percent by volume for

Mach 7 flight simulation. An attempt was made to reduce these levels by decreasing the total enthalpy of the air exiting the heater. This was accomplished by increasing the main airflow rate above the nominal value while keeping the power supply tap settings constant and adjusting the bypass airflow rate to maintain a constant test total enthalpy for a particular throat. With power supply tap settings of 33, data from both the 2.2 in. and the 5.6 in. diameter throats showed only a slight decrease in nitrogen oxide level as main airflow was increased, and therefore, heater flow total temperature was decreased. Similar data for the 1.3 in. diameter throat were not obtained because of arc stability problems. Results are shown in figure 27 for tap settings on both power supplies of 16. Only the Mach 7 data (1.3 in. diameter throat) show a dramatic decrease (56.5 percent) in nitrogen oxide content as the main airflow rate is increased (32 percent). However, in future scramjet tests, this large variation can be used to assess the effect of nitrogen oxide content in the test air on engine performance.

Concluding Remarks

The arc heater research test series showed the versatility of the arc heater and electrical system combination of the Scramjet Test Facility. For scramjet engine testing, the potential of the facility was demonstrated for simulating flight conditions from Mach 4 (at altitudes from 77,000 to 114,000 ft.) to Mach 7 (at altitudes from 108,000 to 149,000 ft.). Arc heater electrical operating characteristics were determined for a wide range of arc power and heater total pressures. Total temperature profiles at the exits of various sized metering nozzles were sufficiently uniform for scramjet engine testing. Levels of nitrogen oxide contaminants in the facility test stream were measured at conditions simulating flight Mach numbers of 4, 5.5, and 7 for use in relating engine test data to expected flight performance.

This test series also provided solutions to some important operational problems, including failure of a critical O-ring and arc instability for some run conditions, which had limited facility productivity in the past. The elimination of these operational problems results in cost savings by minimizing hardware damage during operation, increasing dependability and consistency of the facility, and significantly increasing facility productivity for any type of test series.

References

1. Henry, John R.; and Anderson, Griffin Y.: Design Considerations for the Airframe-Integrated Scramjet. NASA TM X-2895, 1973.

2. Jones, Robert A.; and Huber, Paul W.: Airframe-Integrated Propulsion System for Hypersonic Cruise Vehicles. ICAS Proceedings 1978 - 11th Congress of the International Council of the Aeronautical Sciences (ICAS), Vol. 1 - Fuel Conservation, Hypersonic Vehicles, Environment Effects, Materials and Structures, Computational Aerodynamics, Wind Tunnels, Flight Testing, Stability and Control, J. Singer and R. Staufenbiel.

3. Trexler, Carl A.; and Souders, Sue W.: Design and Performance at a Local Mach Number of 6 of an Inlet for an Integrated Scramjet Concept. NASA TN D-7944, Aug. 1975.

4. Trexler, C. A.: Inlet Performance of the Integrated Langley Scramjet Module (Mach 2.3 to 7.6). Presented at the AIAA/SAE 11th Propulsion Conference, Anaheim, CA, Sept. 1975.

5. McClinton, C. R.; and Gooderum, P. B.: Direct-Connect Test of a Hydrogen-Fueled Three-Strut Injector for an Integrated Modular Scramjet Engine. Presented at the 14th JANNAF Combustion Meeting, Colorado Springs, CO, Aug. 1977.

6. Northam, G. B.; Trexler, C. A.; and McClinton, C. R.: Flameholding Characteristics of a Swept-Strut H_2 Fuel-Injector for Scramjet Applications. Presented at the 17th JANNAF Combustion Meeting, Hampton, VA, Sept. 1980.

7. Andrews, E. H.; Northam, G. B.; Torrence, M. G.; and Trexler, C. A.: Mach 4 Tests of a Hydrogen-Burning Airframe-Integrated Scramjet. Presented at the 18th JANNAF Combustion Meeting, Pasadena, CA, Oct. 1981.

8. Guy, Robert W.; and Mackley, Ernest A.: Initial Wind Tunnel Tests at Mach 4 and 7 of a Hydrogen Burning Airframe-Integrated Scramjet. NASA paper presented at the 4th International Symposium on Air Breathing Engines, Lake Buena Vista, FL, Apr. 1979.

9. Guy, Robert W.; Torrence, Marvin G.; Sabol, Alexander P.; and Mueller, James N.: Operating Characteristics of the Langley Mach 7 Scramjet Test Facility. NASA TM 81929, Mar. 1981.

10. Boatright, William B.; Sabol, Alexander P.; Sebacher, Daniel I.; Pinckney, Shimer Z.; and Guy, Robert W.: Langley Facility for Tests at Mach 7 of Subscale, Hydrogen Burning Airframe-Integratable, Scramjet Models. AIAA Paper No. 76-11, Jan. 1976.

11. Hirsh, Merle N.; and Oskan, M. J. (edited by): Gaseous Electronics, Vol. 1, Electrical Discharges, Academic Press., c. 1978.

12. Beach, H. L., Jr.; Mackley, E. A.; Rogers, R. C.; and Chinitz, W.: Use of Silane in Scramjet Research. Presented at the 17th JANNAF Combustion Meeting, Hampton, VA, Sept. 1978.

13. Moffatt, Robert J.: Gas Temperature Measurement. Temperature - Its Measurement and Control in Science and Industry, Vol. 3, Pt. 2, Reinhold Pub. Corp., c. 1962, pp. 553-571.

14. Slack, M.; and Grillo, A.: Investigation of Hydrogen-Air Ignition Sensitized by Nitric Oxide and by Nitrogen Dioxide. NASA CR-2890, Oct. 1977.

15. Orth, R. C.; Billig, F. S.; and Grenleski, S. E.: Measurement Techniques for Supersonic Combustion Testing. AIAA Progress in Astronautics and Aeronautics, Vol. 34, Jan. 1974.

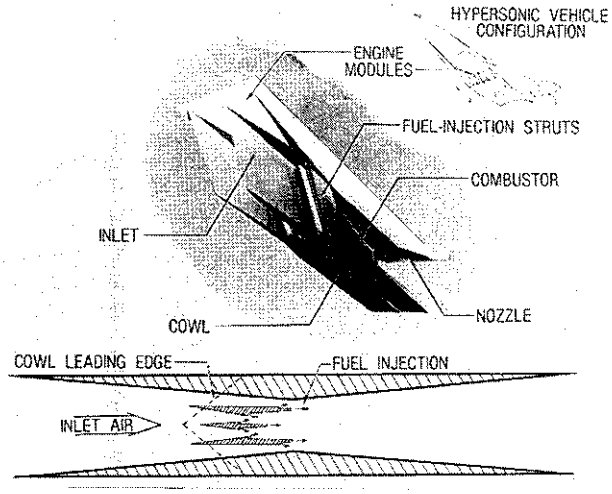

Fig. 1 Airframe-integrated supersonic combustion ramjet.

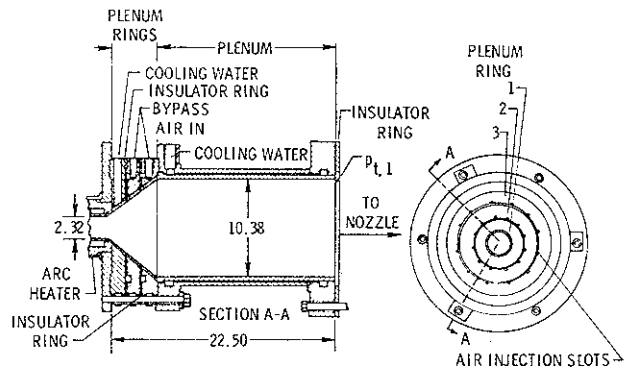

Fig. 4 Section view of the bypass air injection rings and plenum chamber. Dimensions are in inches.

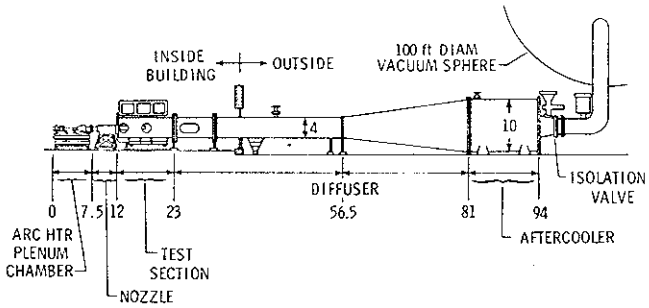

Fig. 2 Elevation view of the Mach 7 Scramjet Test Facility. Dimensions are in feet.

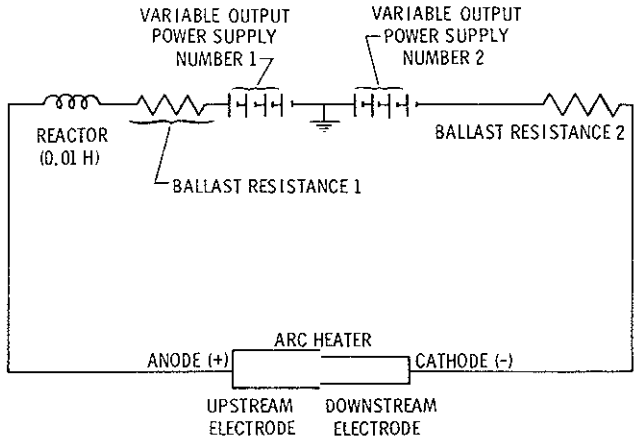

Fig. 5 Arc heater electrical system.

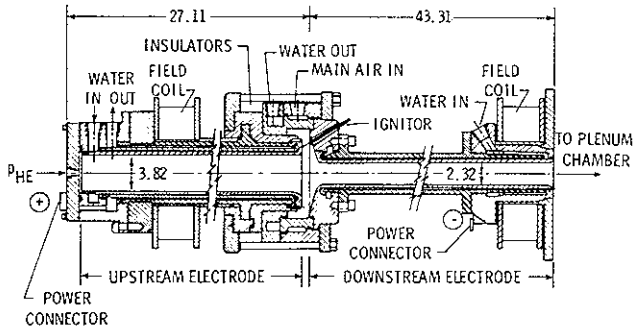

Fig. 3 Section view of the vortex-stabilized arc heater. Dimensions are in inches.

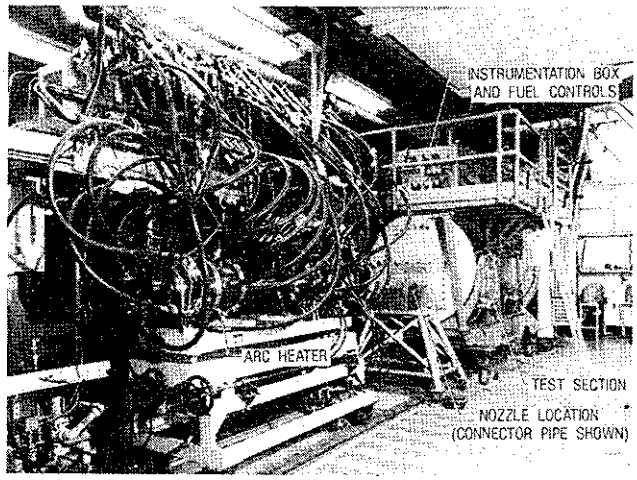

Fig. 6 Photograph of the facility after modification.

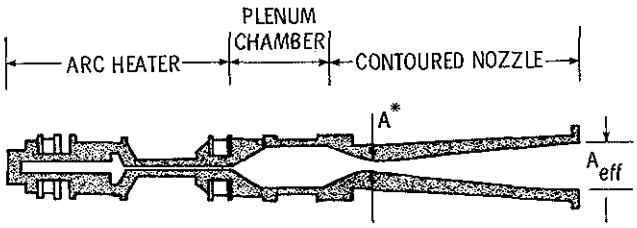

M_∞	M_1	A^* (in.^{2})	A_{eff} (in.^{2})
4.0	3.4	24.63	160
5.5	4.9	3.80	104
7.0	6.0	1.33	104

Fig. 7 Approximate specifications for facility contoured nozzles.

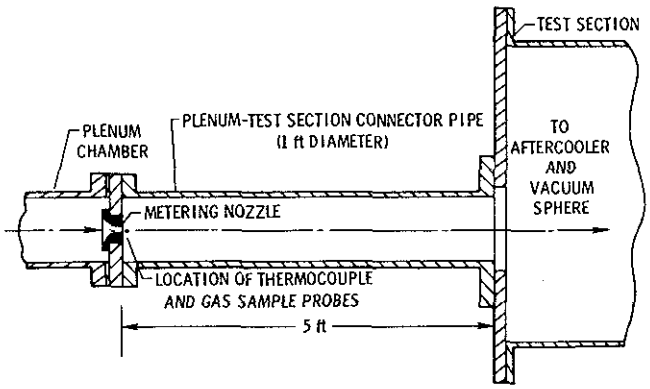

Fig. 8 Test set-up for the arc heater research test series.

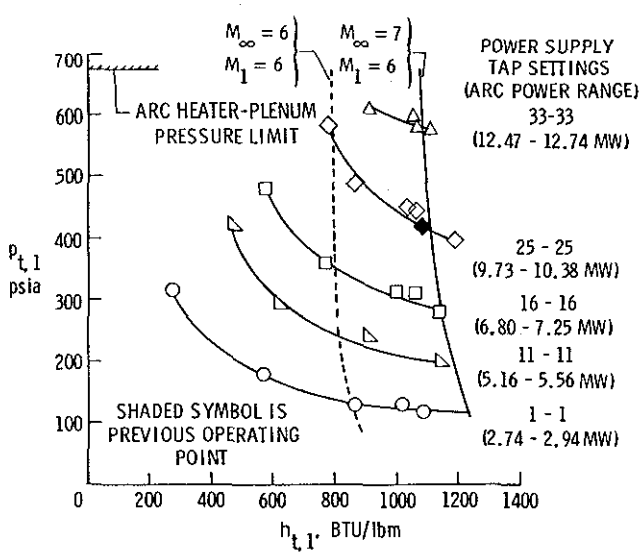

Fig. 9 Facility operating range with a 1.3 inch diameter throat.

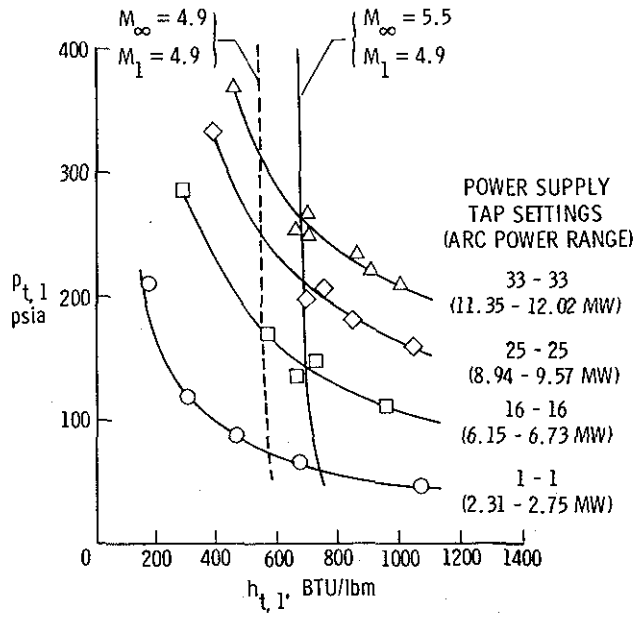

Fig. 10 Facility operating range with a 2.2 inch diameter throat.

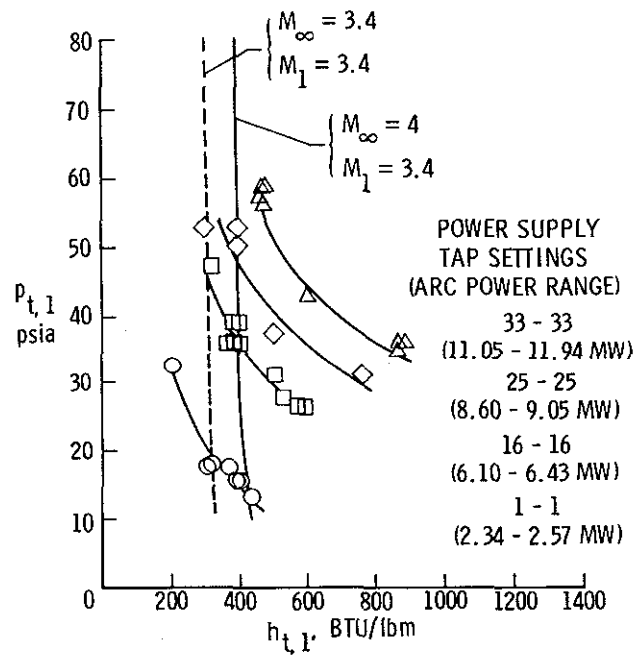

Fig. 11 Facility operating range with a 5.6 inch diameter throat.

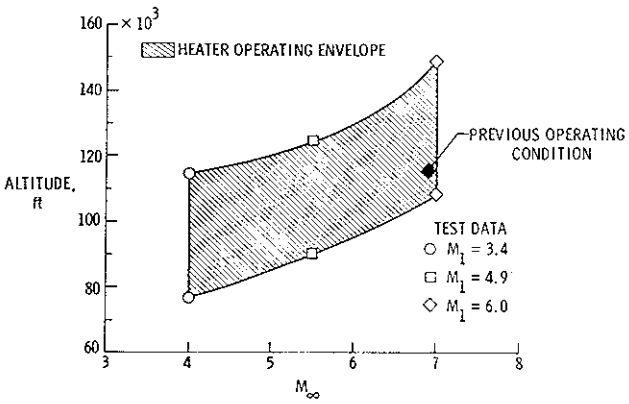

Fig. 12 New STF scramjet engine test envelope.

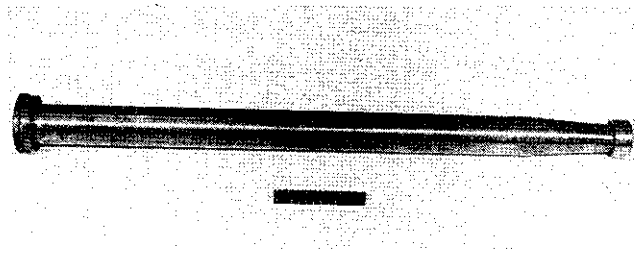

Fig. 15 Photograph of the new, constricted downstream electrode tip.

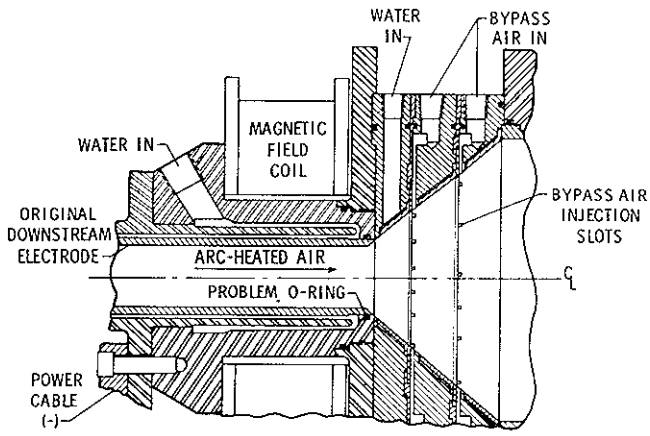

Fig. 13 Schematic of the original downstream electrode tip.

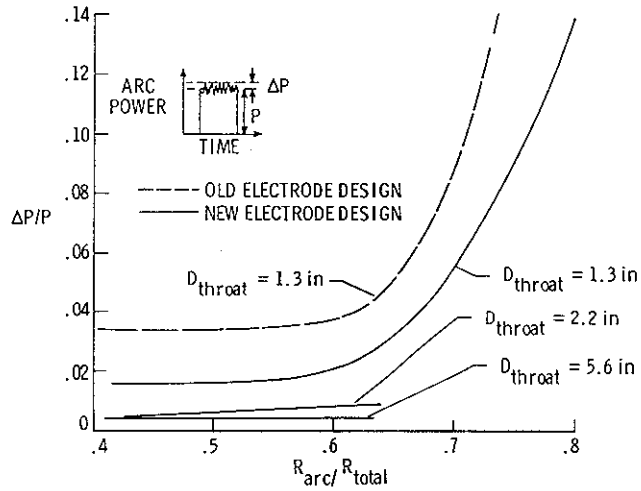

Fig. 16 Normalized arc power fluctuations as a function of arc-to-total resistance ratio.

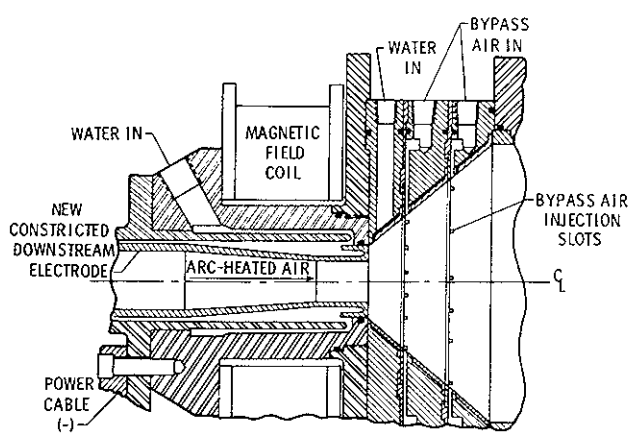

Fig. 14 Schematic of the new, constricted downstream electrode tip.

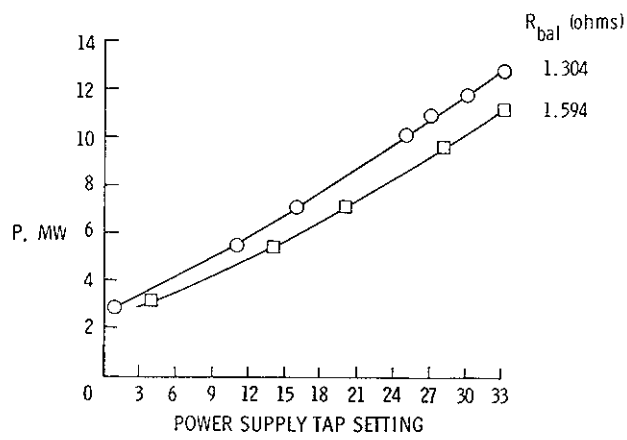

Fig. 17 Effect of ballast resistance on arc power. (1.3 inch diameter throat and nominal airflow rates.)

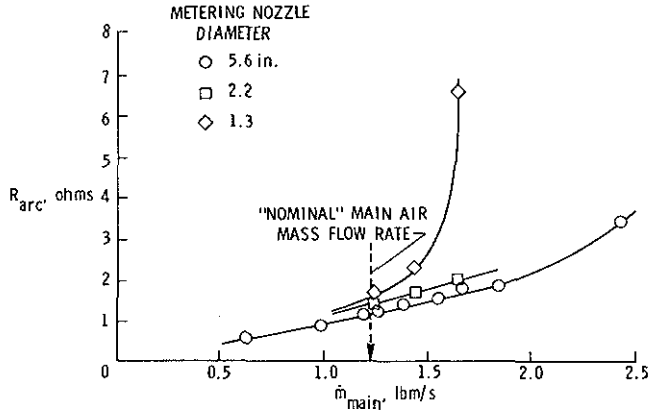

Fig. 18 Variation of arc resistance with arc heater airflow rate and nozzle throat size. (Power supply tap settings of 16 and R_{bal} = 1.304 ohms.)

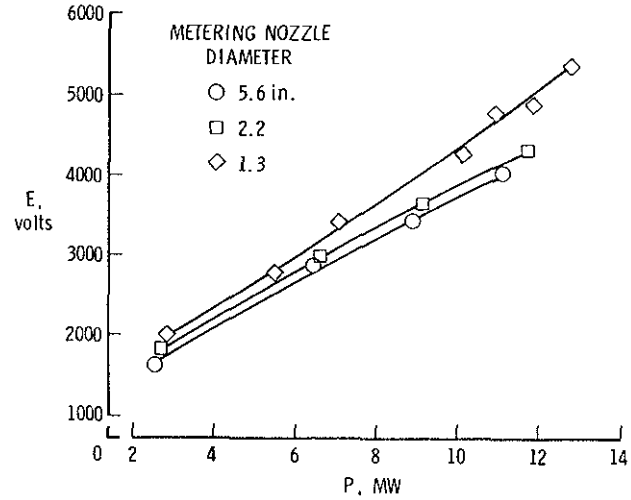

Fig. 21 Arc voltage versus arc power. (R_{bal} = 1.304 ohms, nominal airflow rates.)

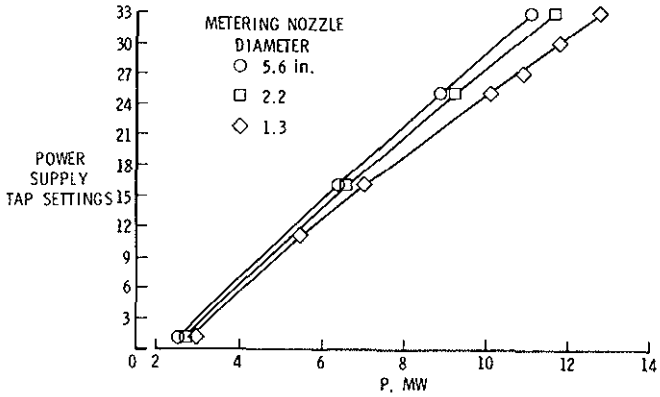

Fig. 19 Power supply tap settings required for various arc power levels. (R_{bal} = 1.304 ohms, nominal airflow rates.)

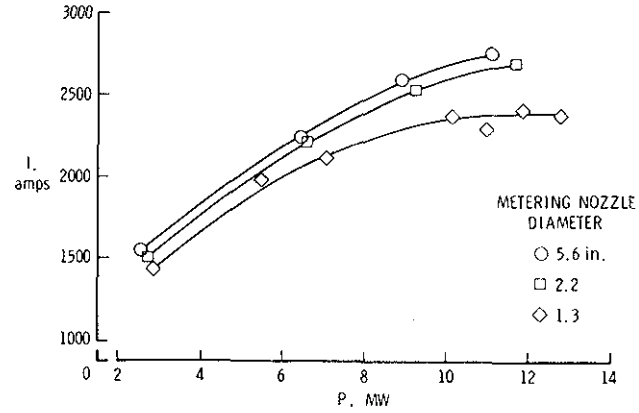

Fig. 22 Arc current versus arc power. (R_{bal} = 1.304 ohms, nominal airflow rates.)

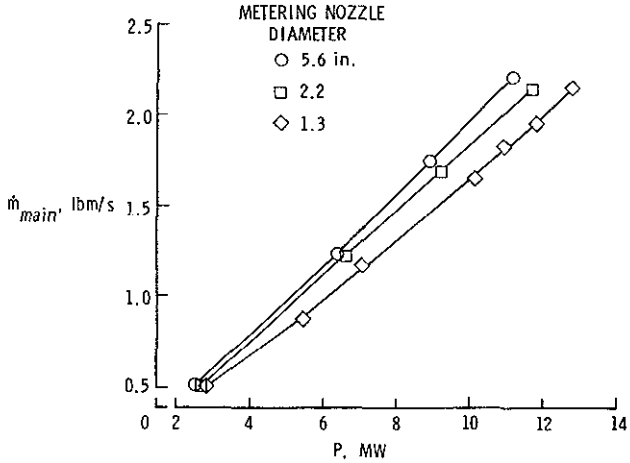

Fig. 20 Nominal main air mass flow rate as a function of arc power.

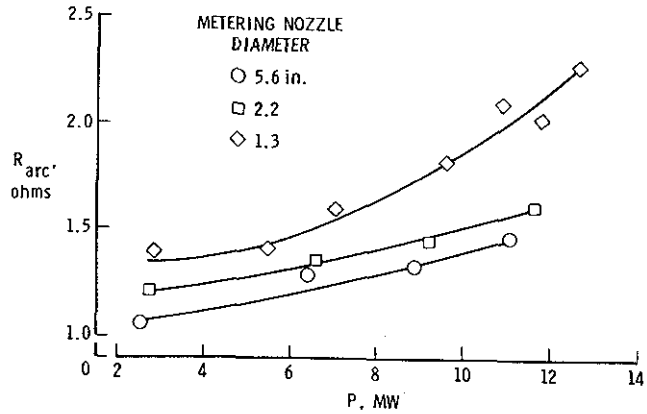

Fig. 23 Arc resistance versus arc power. (R_{bal} = 1.304 ohms, nominal airflow rates.)

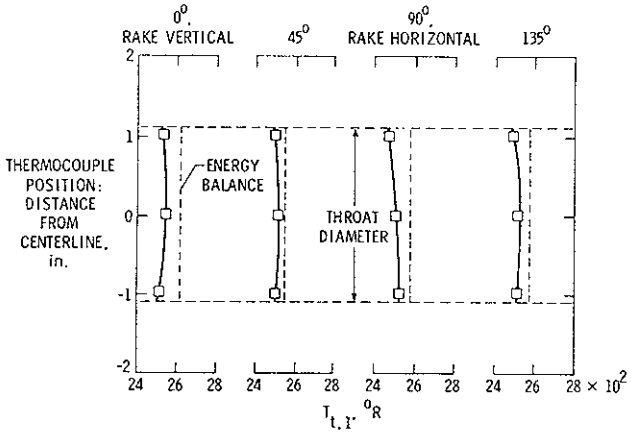

Fig. 24 Total temperature profiles at the exit of the 2.2 inch diameter metering nozzle.

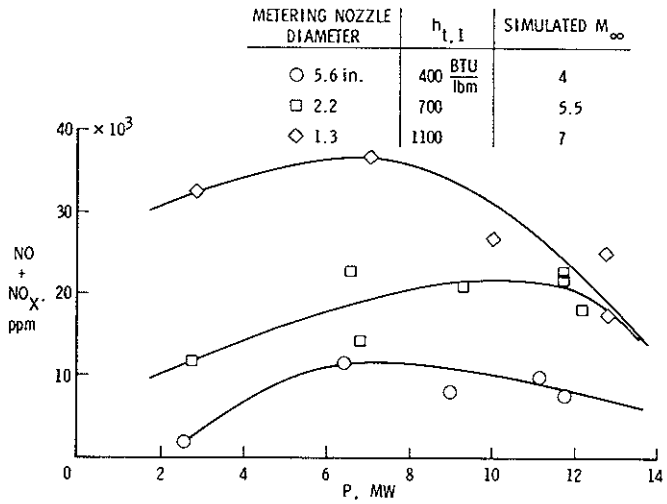

Fig. 26 Nitrogen oxide contaminants in the facility test stream for the range of simulated flight conditions.

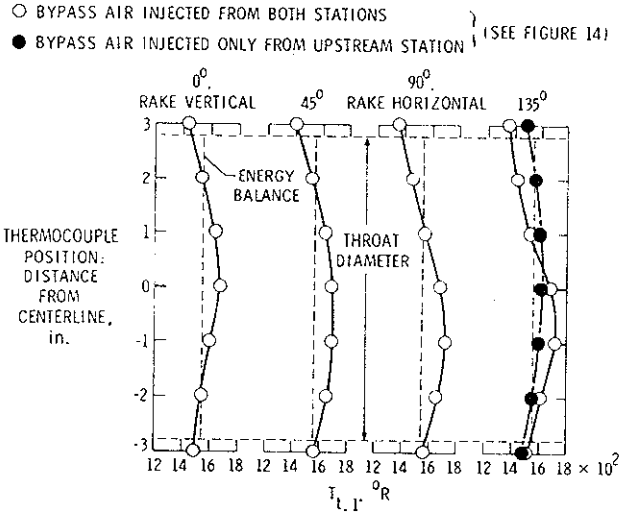

Fig. 25 Total temperature profiles at the exit of the 5.6 inch diameter metering nozzle.

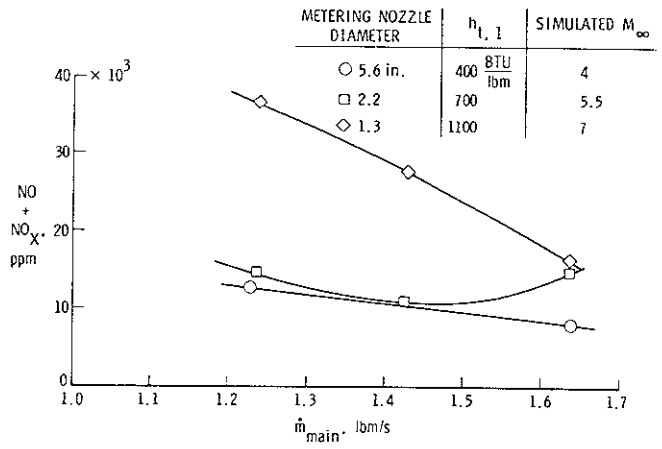

Fig. 27 Effect of arc heater airflow rate on nitrogen oxide contaminent level. (Power supply tap settings of 16.)